U.S. Department of the Interior
U.S. Geological Survey

Seismicity of the Earth 1900–2010

Middle East and Vicinity

Compiled by Jennifer Jenkins,[1] Bethan Turner,[1] Rebecca Turner,[1] Gavin P. Hayes,[2] Alison Sinclair,[1] Sian Davies,[1] Amy Parker,[1] Richard L. Dart, [2] Arthur C. Tarr,[2] Antonio Villaseñor,[3] and Harley M. Benz[2]

2013

[1]Department of Earth and Ocean Sciences, University of Liverpool, Liverpool, United Kingdom
[2]U.S. Geological Survey
[3]Institute of Earth Sciences, CSIC, Barcelona, Spain

Open-File Report 2010–1083–K
Version 1.1, revised January 28, 2014

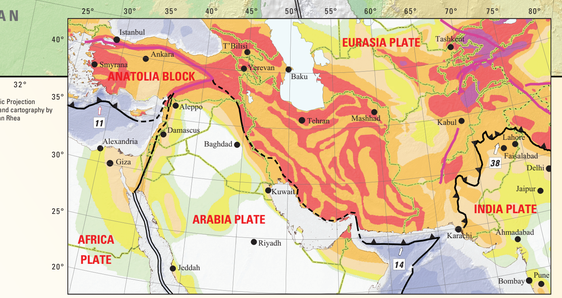

Seismic Hazard and Relative Plate Motion

Scale 1: 28 300 000
0 300 600 900 1200 KILOMETERS

Albers Equal Area Conic Projection
Digital Map database and cartography by Arthur C.Tarr and Susan Rhea

Scale 1: 7 000 000
0 100 200 400 600 800 KILOMETERS

FIGURE EXPLANATION

Peak ground acceleration
0–0.2 m/s²
0.2–0.4
0.4–0.8
0.8–1.6
1.6–3.2
3.2–6.4
6.4–9.8

Plate boundaries
Subduction
Transform
Divergent
Others

Relative plate motion in mm/yr
67

Large Active Fault
Country Boundary

MAP EXPLANATION

Magnitude classes
4–5.9
6–6.4
6.5–6.9
7–7.4
7.5
7.6
7.7
7.8
7.9
8.0
8.1
8.2

Depth of focus
0–69 km
70–299 km
300–700 km

Plate boundaries
Subduction
Transform
Divergent
Others

Active volcanoes
Large Active Fault
Country Boundary

TECTONIC SUMMARY

No fewer than four major tectonic plates (Arabia, Eurasia, India, and Africa) and one smaller tectonic block (Anatolia) are responsible for seismicity and tectonics in the Middle East and surrounding region. Geologic development of the region is a consequence of a number of first-order plate tectonic processes that include subduction, large-scale transform faulting, compressional mountain building, and crustal extension.

Mountain building in northern Pakistan and Afghanistan is the result of compressional tectonics, associated with collision of the India plate moving northwards at a rate of 40 mm/yr with respect to the Eurasia plate. Continental thickening of the northern and western edge of the India subcontinent has produced the highest mountains in the world, including the Himalaya, Karakorum, Pamir and Hindu Kush ranges. Earthquake activity and faulting found in this region, as well as adjacent parts of Afghanistan and India, are due to collisional plate tectonics.

Beneath the Pamir–Hindu Kush Mountains of northern Afghanistan, earthquakes occur to depths as great as 200 km as a result of remnant lithospheric subduction. Shallower crustal earthquakes in the Pamir–Hindu Kush Mountains occur primarily along the Main Pamir Thrust and other active Quaternary faults, which accommodate much of the region's crustal shortening. The western and eastern margins of the Main Pamir Thrust display a combination of thrust and strike-slip mechanisms.

Along the western margin of the Tibetan Plateau, in the vicinity of southeastern Afghanistan and western Pakistan, the India plate translates obliquely relative to the Eurasia plate, resulting in a complex fold-and-thrust belt known as the Sulaiman Range. Faulting in this region includes strike-slip, reverse-slip and oblique-slip motion and often results in shallow, destructive earthquakes. The relatively fast moving left-lateral, strike-slip Chaman Fault system in southeastern Afghanistan accommodates translational motion between the India and Eurasia plates. In 1505, a segment of the Chaman Fault system near Kabul, Afghanistan, ruptured causing widespread destruction of Kabul and surrounding villages. In the same region, the more recent May 30, 1935, M7.6 Quetta, Pakistan, earthquake occurred within the Kirthar range, killing between 30,000 and 60,000 people.

Off the south coast of Pakistan and southeast coast of Iran, the Makran trench is the present-day surface expression of active subduction of the Arabia plate beneath the continental Eurasia plate, which converge at a rate of approximately 20 mm/yr. Although the Makran subduction zone has a relatively slow convergence rate, it has produced large devastating earthquakes and tsunamis. For example, the November 27, 1945, M8.0 mega-thrust earthquake produced a tsunami within the Gulf of Oman and Arabian Sea, killing over 4,000 people. Northwest of this active subduction zone, collision of the Arabia and Eurasia plates forms the approximately 1,500-km-long fold and thrust belts of the Zagros Mountains, which crosses the whole of western Iran and extends into northeast-ern Iraq. Collision of the Arabia and Eurasia plates also causes crustal shortening in the Alborz Mountains and Kopet Dag in Northern Iran. Eastern Iran undergoes destructive earthquakes that originate on both strike-slip and reverse faults. For example, the September 16, 1978, M7.4 earthquake, along the northwest edge of the Dasht-e-Lut Basin, killed at least 15,000 people. Though smaller, the M6.5 December 26, 2008, Bam earthquake, near the southwestern edge of the Dasht-e-Lut Basin, resulted in over 25,000 deaths.

Along the eastern margin of the Mediterranean region there is complex interaction among Africa, Arabia, and Eurasia plates. The Red Sea Rift is a spreading center between the Africa and Arabia plates, with a spreading rate of approximately 10 mm/yr near its northern end, and 16 mm/yr near its southern end (Chu and Gordon, 1998). Seismicity rate and size of earthquakes has been relatively small along the spreading center, but the rifting process has produced a series of volcanic systems across western Saudi Arabia.

Further north, the Red Sea Rift terminates at the southern boundary of the Dead Sea Transform Fault. The Dead Sea Transform is a strike-slip fault that accommodates differential motion between the Africa and Arabia plates. Though both the Africa plate, to the west, and the Arabia plate, to the east, are moving in a NNE direction, the Arabia plate is moving slightly faster, resulting in the left-lateral, strike-slip motion along this segment of the plate boundary. Historically, earthquake activity along the Dead Sea Transform has been a significant hazard in the densely populated Levant region (eastern Mediterranean). For example, the November 1759 Near East earthquake is thought to have killed somewhere between 2,000–20,000 people. The northern termination of the Dead Sea Transform occurs within a complex tectonic region of southeast Turkey, where interaction of the Africa and Arabia plates and the Anatolia block occurs. This involves translational motion of the Anatolia block westwards, with a speed of approximately 25 mm/yr with respect to Eurasia, in order to accommodate closure of the Mediterranean Basin.

The right-lateral, strike-slip North Anatolia Fault, in northern Turkey, accommodates much of the westwards motion between the Anatolia block and Eurasia plate. Between 1939 and 1999, a series of devastating M7.0+ strike-slip earthquakes propagated westward along the North Anatolia Fault system. The westernmost of these earthquakes was the August 17, 1999, M7.6 Izmit earthquake, near the Sea of Marmara, which killed approximately 17,000 people.

At the southern edge of the Anatolia block lies the east-west trending Cyprian Arc with associated levels of moderate seismicity. The Cyprian Arc represents the convergent boundary between the Anatolia block to the north and the Africa plate to the south. The boundary is thought to join the East Anatolia Fault zone in eastern Turkey; however, no certain geometry or sense of relative motion along the entire boundary is widely accepted.

DATA SOURCES

The earthquake locations shown on the main map (left) are taken from the global 1900–2007 Centennial Catalog (Engdahl and Villaseñor, 2002), a catalog of high-quality depth determinations for the period 1964–2002 (Engdahl, personal commun., 2003), and U. S. Geological Survey-Preliminary Determination of Epicenters (USGS-PDE, *http://earthquake.usgs.gov/research/data/pde.php*) for the years 2008–2010.

Major earthquakes (7.5≤M≤8.2) are labeled with the year of occurrence, while earthquakes (8.0≤M≤8.2) are labeled with the year of occurrence and also denoted by a white outline (Tarr and others, 2010).

The Seismic Hazard and Relative Plate Motion figure (lower left) shows the generalized seismic hazard (Giardini and others, 1999) and relative plate motion vectors (open arrows with labels) using the Morvel model (DeMets and others, 1994).

Base map data sources include GEBCO 2008 shaded relief, Volcanoes of the World dataset (Siebert and Simkin, 2002); plate boundaries (Bird, 2003); and geographic information from Digital Chart of the World (1992), and ESRI (2002).

REFERENCES

Bird, Peter, 2003, An updated digital model of plate boundaries: Geochemistry Geophysics Geosystems, v. 4, no. 3, 52 p.

Chu, D., Gordon, R.G., 1998, Current plate motions across the Red Sea: Geophysical Journal International, v. 135, is. 2, p. 313–328.

Daëron, M., Klinger, Y., Tapponnier, P., Elias, A., Jacques, E., and Sursock, A., 2005, Sources of the large A.D. 1202 and 1759 Near East earthquakes: Geology, v. 35, p. 755–758, doi:10.1130/G23631A.1.

DeMets, Charles, Gordon, R.G., Argus, D.F., and Stein, Seth, 1994, Effect of recent revisions to the geomagnetic time scale on estimates of current plate motions: Geophysical Research letters, v. 21, p. 2191–2194.

Digital Chart of the World, 1992: Accessed on Mar. 9, 1996 at *http://earth-info.nga.mil/publications/specs/printed/89009/89009_DCW.pdf*.

Engdahl, E.R., and Villaseñor, Antonio, 2002, Global seismicity 1900–1999, *in* Lee, W.H.K., Kanamori, Hiroo, Jennings, P.C., and Kisslinger, Carl, eds., International Handbook of Earthquake and Engineering Seismology, v. 81(A), chap. 41, p. 1–26.

ESRI, 2002, ESRI data and maps: Redlands, Calif., ESRI. Available at *http://www.esri.com/data/data-maps*.

GEBCO, 2008, The GEBCO_08_Grid, ver. 20091120: GEBCO. Accessed Jan. 8, 2010 at *http://www.gebco.net*.

Giardini, D., Grunthal, G., Shedlock, K., Zhang. P., and Global Seismic Hazards Program, 1999, Global seismic hazards map: Accessed on Jan. 9, 2007 at *http://www.seismo.ethz.ch/GSHAP*.

National Oceanic and Atmospheric Administration (NOAA), 2010: National Geophysical data Center (NGDC): National Oceanic and Atmospheric Administration, Accessed on Mar. 31, 2010 at *http://www.ngdc.noaa.gov/ngdc.html*.

Siebert, Lee, and Simkin, Thomas, 2002, Volcanoes of the world—An illustrated catalog of Holocene volcanoes and their eruptions: Smithsonian Institution, Global Volcanism Program Digital Information Series, GVP-3. Accessed on Jan. 9, 2007 at *http://www.volcano.si.edu/world*.

Tarr, A.C., Villaseñor, Antonio, Furlong, K.P., Rhea, Susan, and Benz, H.M., 2010, Seismicity of the Earth 1900–2007: U.S. Geological Survey Scientific Investigations Map 3064, scale 1:25,000,000. Available at *http://pubs.usgs.gov/sim/3064*.

Publishing support provided by:
Denver Publishing Service Center
Manuscript approved for publication January 4, 2013

Suggested citation:
Jenkins, Jennifer, Turner, Bethan, Turner, Rebecca, Hayes, G.P., Sinclair, Alison, Davies, Sian, Parker, Amy, Dart, R.L., Tarr, A.C., Villaseñor, Antonio, and Benz, H.M., compilers, 2013, Seismicity of the Earth 1900–2010 Middle East and vicinity (ver. 1.1, Jan. 28, 2014): U.S. Geological Survey Open-File Report 2010–1083–K, scale 1:7,000,000, *http://pubs.usgs.gov/of/2010/1083/k/*.